Tuning organic ligands to optimize the nitrogen reduction performance of Co(II) or Ni(II)-based MOFs

Ling Qin[*,a,b], Ying-Xin Zhao[a], Qiang Liu[a], Jin-Long An[a], Han-Xi Wang[a], Mao-Feng Zhang[a], Cheng-Wu Shi[a], He-Gen Zheng[*, c]

[a]*School of Chemistry and Chemical Engineering, Hefei University of Technology, Hefei, 230009, Anhui, P. R. China.*

[b]*School of Materials Science and Engineering, Hefei University of Technology, Hefei, 230009, Anhui, P. R. China.*

[c]*State Key Laboratory of Coordination Chemistry, School of Chemistry and Chemical Engineering, Collaborative Innovation Center of Advanced Microstructures, Nanjing University, Nanjing 210023, P. R. China.*

*Corresponding author. E-mail: qinling@hfut.edu.cn; zhenghg@nju.edu.cn

1. Experiment

1.1 Materials

Sodium salicylate ($C_7H_5O_3N$, 99.5%, Beijing Innochem Technology Co.); sodium hypochlorite (NaClO, >10% active chlorine, innochem); sodium nitroferricyanide dihydrate ($C_5FeN_6Na_2O{\cdot}2H_2O$, 99%, innochem); ammonium chloride (NH_4Cl, 99.5%, innochem), hydrazine monohydrochloride (ClH_5N_2, 98%, innochem); 4-(dimethylamino) benzaldehyde ($C_9H_{11}NO$, 99%, innochem); potassium sodium tartrate tetrahydrate ($C_4H_4O_6KNa{\cdot}4H_2O$, 99.5%, innochem); N,N-dimethylformamide (C_3H_7NO, AR, 99.5%, innochem); ethanol (C_2H_6O, AR, innochem); N,N-

dimethylacetamide (C_4H_9NO, 99.9%, innochem); cobalt nitrate hexahydrate ($Co(NO_3)_2·6H_2O$, 99%, Shanghai Aladdin Biochemical Technology Co.); nickel nitrate hexahydrate ($Ni(NO_3)_2·6H_2O$, 98%, Sinopharm Group Chemical Reagent Co.); hydrochloric acid (HCl, 37%, Sinopharm Group Chemical Reagent Co.); sulfuric acid (H_2SO_4, 98%, Sinopharm Group Chemical Reagent Co.); hydrogen peroxide (H_2O_2, 30%, Sinopharm Group Chemical Reagent Co.); acetone (C_3H_6O, 99.5%, Sinopharm Group Chemical Reagent Co.); nitric acid (HNO_3, 68%, Sinopharm Group Chemical Reagent Co.); anhydrous sodium sulfate (Na_2SO_4, 99%, Beijing Innochem Technology Co.); nessler reagent (K_2HgI_4, AR, innochem); 2,5-bis(4-pyridyl)-1,3,4-thiadiazole ($C_{12}H_8N_4S$, 97%, Jinan Henghua Technology Co.); 1,4-di(pyridin-4-yl)benzene ($C_{16}H_{12}N_2$, 97%, Shanghai Adamas Reagent Co.); 3,5-bis(pyridine-4-yl)-4-amino-1,2,4-triazole ($C_{12}N_6H_{10}$, 97%, Jinan Henghua Technology Co.); 3,6-bis(4'-pyridyl)-1,2,4,5-tetrazine ($C_{12}N_6H_8$, 97%, Henghua); 4,4'-dithiodipyridine ($C_{10}H_8N_2S_2$, 98%, Extension); Nafion solution (5 wt%, Shanghai Macklin Biochemical Technology Co.); carbon cloth (WOS1011, Suzhou zhengtai Rongxin Material Co.). All reagents are of analytical reagent grade and do not require further purification.

1.2 Characterization instrument

X-ray diffraction (XRD) is measured on a fixed target X-ray diffractometer (PANalytical X-Pert PRO MPD) using Cu-Kα radiation (1.5418 Å). The microscopic morphology of the sample is tested by thermal field emission scanning electron microscope (SEM, Gemini 500). X-ray photoelectron spectrum (XPS) measurement was performed on ESCALAB250Xi spectrometer (Thermo) using Al Kα radiation.

BET measurement was performed on ASAP 2460 series multi-station extended automatic specific surface area and porosity analyzer.

1.3 Preparation

1.3.1 Preparation of Ni-dpt-H_2tdc:

The preparation of Ni-dpt-H_2tdc is similar to that of Co-dpt-H_2tdc, except that $Co(NO_3)_2 \cdot 6H_2O$ is replaced by $Ni(NO_3)_2 \cdot 6H_2O$.

1.3.2 Preparation of Ni-bptz-H_2tdc:

The preparation of Ni-bptz-H_2tdc is similar to that of Co-bptz-H_2tdc, except that $Co(NO_3)_2 \cdot 6H_2O$ is replaced by $Ni(NO_3)_2 \cdot 6H_2O$.

1.3.3 Preparation of Ni-bpat-H_2tdc

The preparation of Ni-bpat-H_2tdc is similar to that of Co-bpat-H_2tdc, except that $Co(NO_3)_2 \cdot 6H_2O$ is replaced by $Ni(NO_3)_2 \cdot 6H_2O$.

1.3.4 Preparation of Ni-dpb-H_2tdc

The preparation of Ni-dpb-H_2tdc is similar to that of Co-dpb-H_2tdc, except that $Co(NO_3)_2 \cdot 6H_2O$ is replaced by $Ni(NO_3)_2 \cdot 6H_2O$.

1.3.5 Preparation of Ni-pds-H_2tdc

The preparation of Ni-pds-H_2tdc is similar to that of Co-pds-H_2tdc, except that $Co(NO_3)_2 \cdot 6H_2O$ is replaced by $Ni(NO_3)_2 \cdot 6H_2O$.

1.4 Electrochemical tests:

We used a H-type electrolytic cell, separated by a Nafion 115 membrane, activated in an aqueous solution of H_2O_2 (5 %), 0.5 M H_2SO_4 and deionized water, respectively, for 1h at 85˚C. A three-electrode system with a carbon cloth as the working electrode,

an Ag/AgCl (filled with saturated KCl solution) as the reference electrode, and a graphite rod as the counter electrode was used for the electrochemical experiments. An electrochemical workstation was used to perform electrochemical experiments in N_2 saturated 0.1 M Na_2SO_4 solution. The potentials reported in this work were converted to reversible hydrogen electrode (RHE) scale by calibration with the equation E (RHE) = E (vs. Ag/AgCl) +0.197+0.059*pH.

Carbon cloth was sonicated with acetone, ethyl alcohol, and deionized water for 20 min each respectively and then soaked in 30 % HNO_3 for 24h, washed with H_2O and dried at 60˚ for 12h.

Table S1 The synthesis conditions and crystal information of ten Co-MOFs and Ni-MOFs.

MOFs	Solvent ratio	Shape	Colour	Yield
Co-dpt-H_2tdc	DMF: H_2O=3:1	prismatic	red	69%
Co-bptz-H_2tdc	DMF: H_2O=1:1	prismatic	red	51%
Co-bpat-H_2tdc	DMA: H_2O=1:1	prismatic	purplish-red	66%
Co-dpb-H_2tdc	DMF: H_2O=1.5:1	needlelike	pink	46%
Co-pds-H_2tdc	DMF: H_2O=2:1	block	pink	63%
Ni-dpt-H_2tdc	DMF: H_2O=3:1	prismatic	green	65%
Ni-bptz-H_2tdc	DMF: H_2O=1:1	prismatic	green	56%
Ni-bpat-H_2tdc	DMA: H_2O=1:1	prismatic	green	62%
Ni-dpb-H_2tdc	DMF: H_2O=1.5:1	needlelike	green	49%
Ni-pds-H_2tdc	DMF: H_2O=2:1	block	blue	60%

1.4.1 Preparation of working electrode:

1 mL of ethyl alcohol and 20 μL of Nafion solution (5 wt%) were added to 5 mg of catalyst, the mixture was sonicated for 30 min. Then 20 μL of the dispersed solution of catalyst was dripped onto the carbon cloth.

1.4.2 Detection of NH_3:

1.4.2.1 Indophenol blue spectrophotometry:

The concentration of NH_3 generated was determined by indophenol blue spectrophotometry. 2 mL of electrolyte was taken from the cathode chamber and 1 mL of oxidizing solution containing NaClO (>10% active chlorine), 2 mL of color developing solution containing sodium salicylate and potassium sodium tartrate tetrahydrate and 0.2 mL of catalyst solution containing sodium nitroferricyanide dihydrate were added, and the reaction was carried out for 1 h. In 0.1 M Na_2SO_4 solution to calibrate the concentration absorption curves with NH_4Cl standard solutions with NH_3 concentrations of 0, 0.1, 0.2, 0.4, 0.8, 1, 1.2, 1.5 and 2 $\mu g \cdot mL^{-1}$. These solutions were characterized by UV-Vis spectroscopy at 655 nm. The concentration-absorption curves were calibrated with a range of concentrations of NH_3 standard solutions. The fitted curve ($y = 0.50339x + 0.0254$, $R^2 = 0.999$) showed a good linear relationship between the absorbance values and NH_3 concentration.

1.4.2.2 Nessler's reagent spectrophotometry:

The concentration of NH_3 generated was also determined by Nessler's reagent spectrophotometry. 25 mL of electrolyte was taken from the cathode chamber, 0.5 mL of potassium tartrate sodium solution was added, stirred well and 0.5 mL of Nasher's

reagent was added dropwise, shaken well, and left to stand for 20 min. The absorbance value-concentration curves were calibrated with NH_4Cl standard solutions in 0.1 M Na_2SO_4 solution with NH_3 concentrations of 0, 0.1, 0.2, 0.4, 0.8, 1.2, 1.6, and 2 $\mu g \cdot mL^{-1}$. These solutions were characterized by UV-visible spectroscopy at 420 nm. The absorbance value-concentration curves were calibrated with a range of concentrations of NH_3 standard solutions. The fitted curve ($y = 0.19148x + 0.01146$, $R^2 = 0.999$) showed a good linear relationship between absorbance values and NH_3 concentration.

1.4.3 Detection of N_2H_4:

The Watt-Chrisp method was used to estimate N_2H_4 production. The color developer was a mixed solution of 5.99 g 4-(dimethylamino) benzaldehyde, 30 mL HCl and 300 mL C_2H_5OH. 5 mL of electrolyte was removed from the electrochemical reaction vessel, 5 mL of prepared color developer was added, and the absorbance of the solution at 455 nm was measured at room temperature for 15 min to quantify the yield of hydrazine by the standard curve of hydrazine ($y = 1.41171x + 0.0119$, $R^2 = 0.998$).

1.4.4 Determination of FE and NH_3:

FE is calculated by the formula:

$$FE = 3 \times F \times [NH_3] \times V / 17 \times Q \times 100\%$$

NH_3 yield is calculated by the formula:

$$NH_3 \text{ yield} = [NH_3] \times V / t \times m$$

F is Faraday constant (96500 $C \cdot mol^{-1}$), $[NH_3]$ is the NH_3 concentration of the electrolyte calculated according to the standard curve ($mg \cdot L^{-1}$); Q is the total amount of electricity

applied, V is the volume of electrolyte (ml); t is the reaction time (h); m is the mass of catalyst (mg).

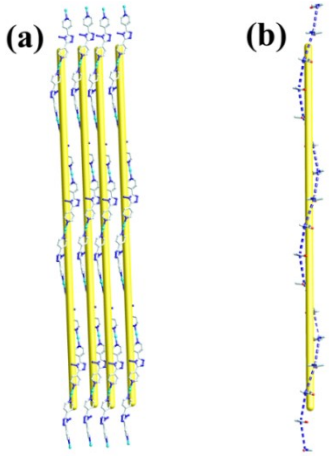

Figure S1 (a) A view of 1D right-helical chain relying on the coordinate interaction between nitrogen and Co ions in Co-bpat-H_2tdc; (b) A view of 1D right-helical DMA helical channel inside the molecular helix in Co-bpat-H_2tdc.

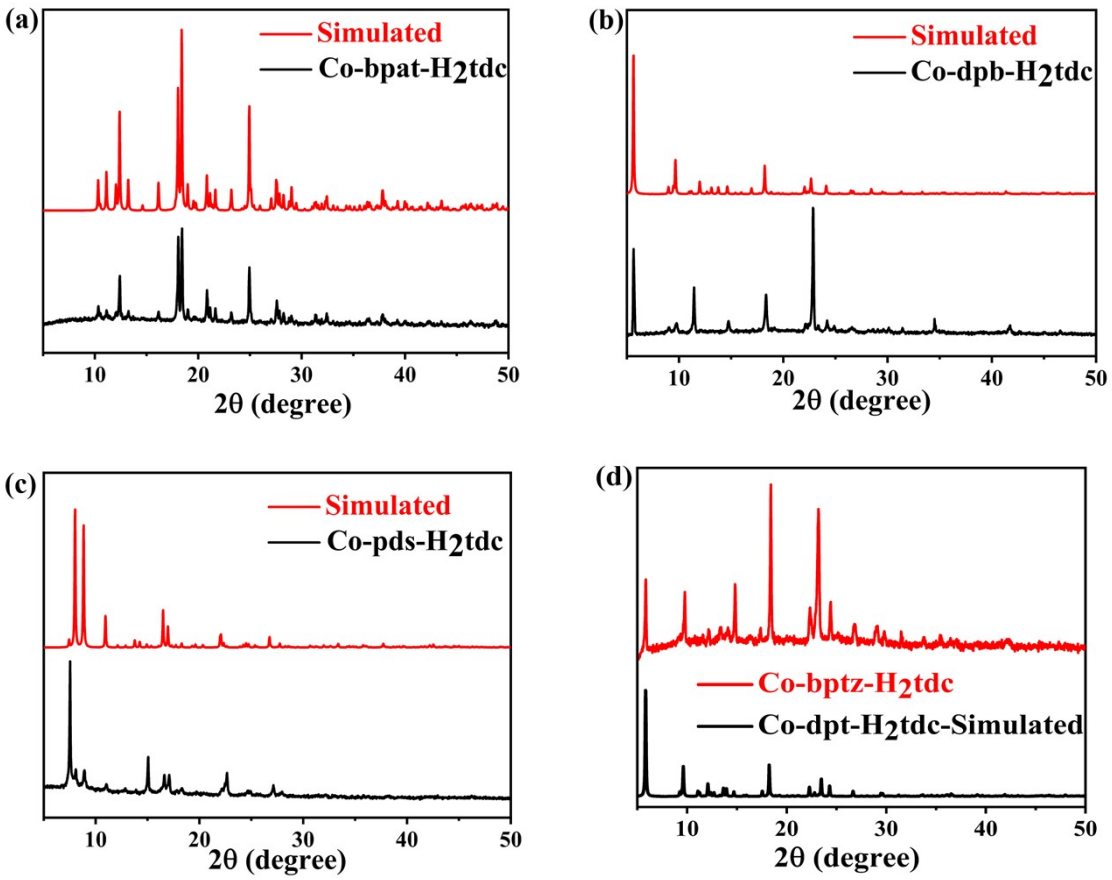

Figure S2 PXRD of synthesized sample and standard spectra simulated by single crystal diffraction data of (a) Co-bpat-H_2tdc, (b) Co-dpb-H_2tdc，(c) Co-pds-H_2tdc, (d) Co-bptz-H_2tdc and standard spectra simulated by Co-dpt-H_2tdc.

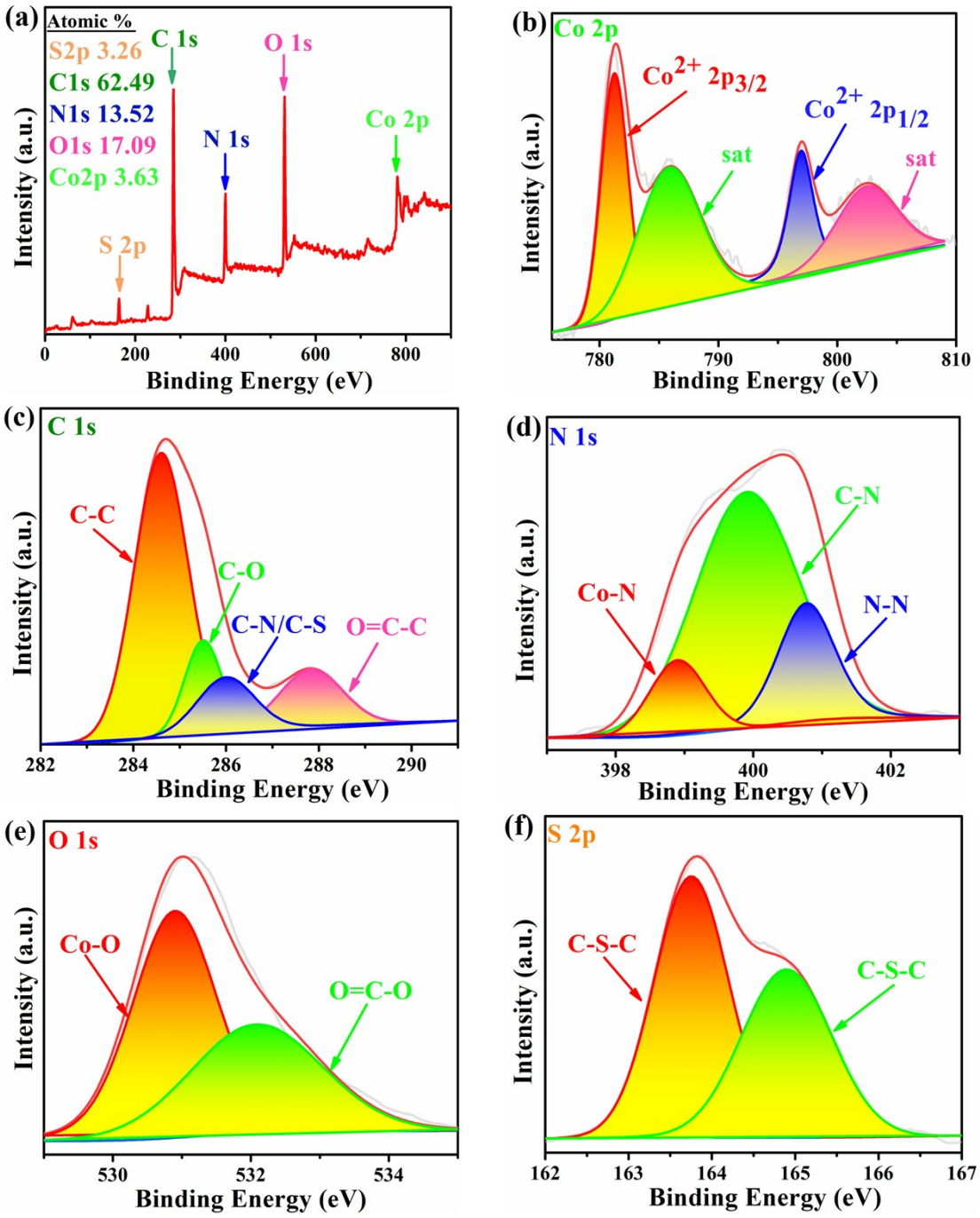

Figure S3 (a) XPS survey of Co-bptz-H_2tdc; (b) Co 2p; (c) C 1s; (d) N 1s; (e) O 1s; (f) S 2p spectrum.

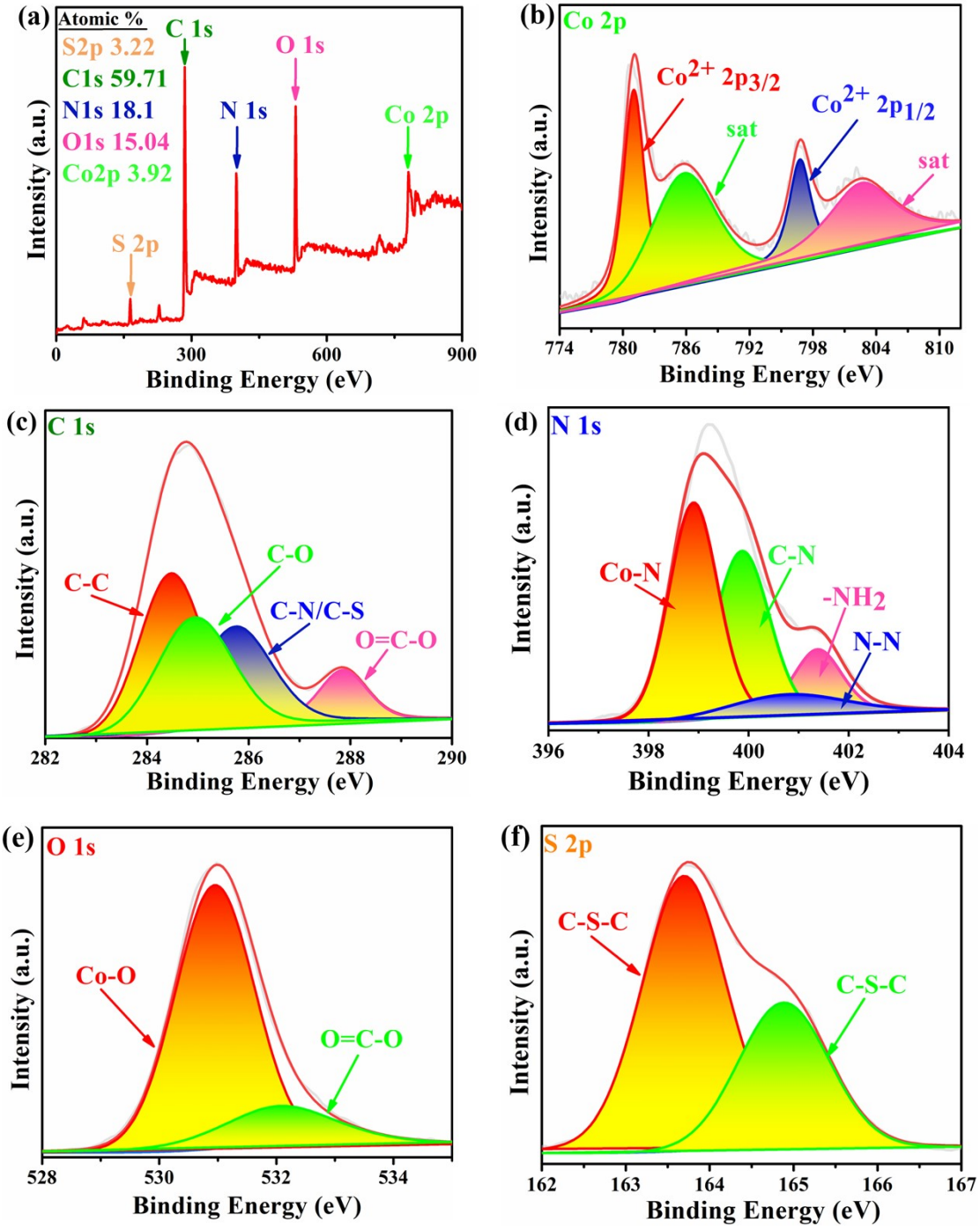

Figure S4 (a) XPS survey of Co-bpat-H_2tdc; (b) Co 2p; (c) C 1s; (d) N 1s; (e) O 1s; (f) S 2p spectrum.

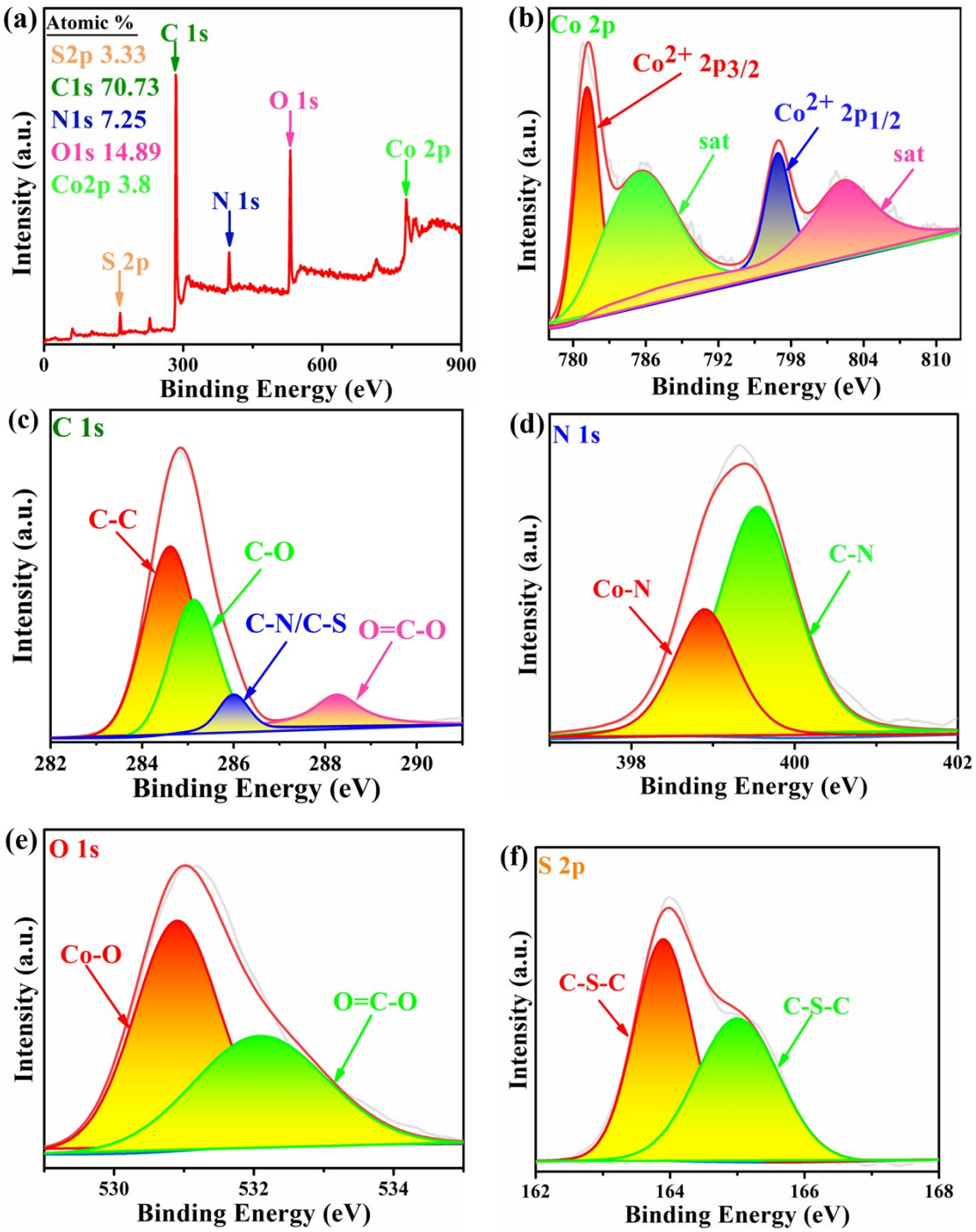

Figure S5 (a) XPS survey of Co-dpb-H_2tdc; (b) Co 2p; (c) C 1s; (d) N 1s; (e) O 1s; (f) S 2p spectrum.

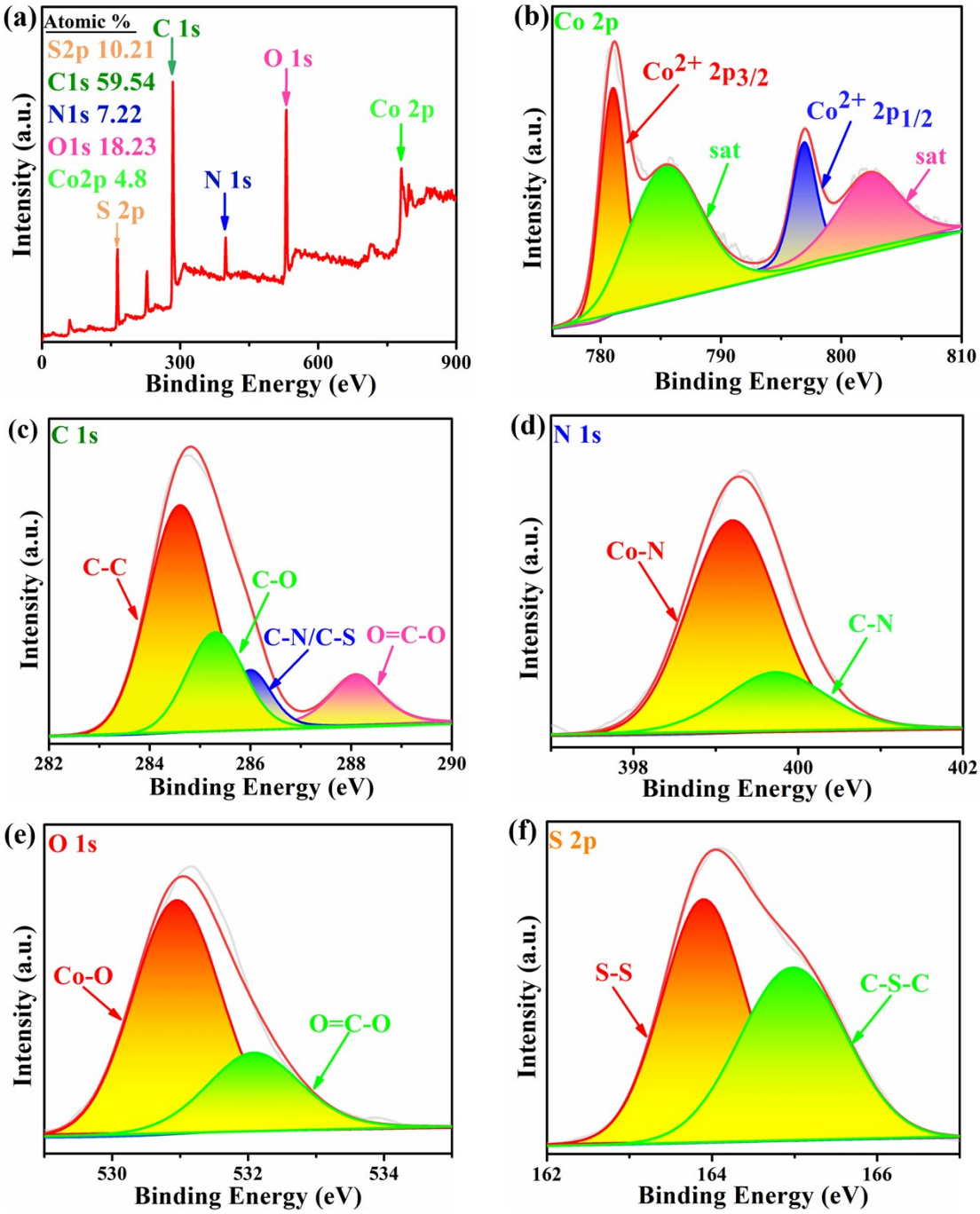

Figure S6 (a) XPS survey of Co-pds-H_2tdc; (b) Co 2p; (c) C 1s; (d) N 1s; (e) O 1s; (f) S 2p spectrum.

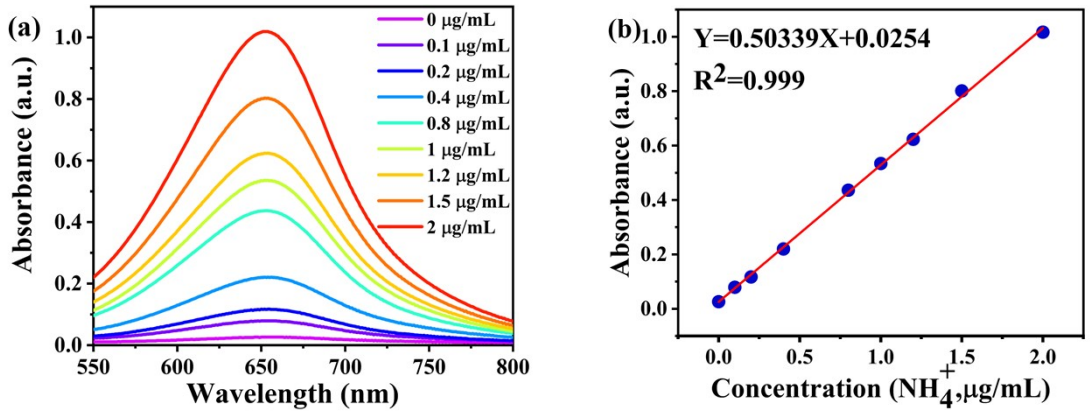

Figure S7 (a) UV absorbance spectrum for quantitative measurement of NH_3 nitrogen by indophenol blue after incubated for 1 h at room temperature; (b) the corresponding calibration curve used for calculation of NH_4^+ concentrations.

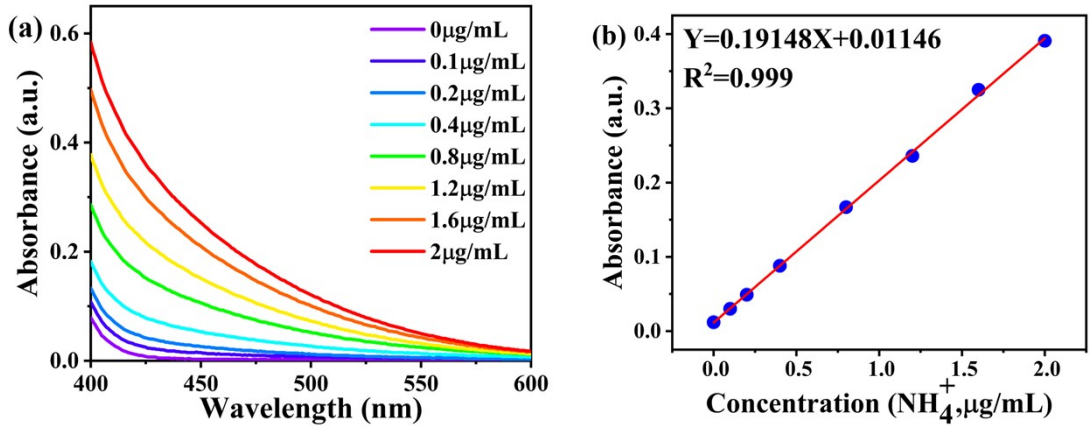

Figure S8 (a) UV absorbance spectrum for quantitative measurement of NH_3 nitrogen by Nessler's Reagent Spectrophotometry after incubated for 20 min at room temperature; (b) the corresponding calibration curve used for calculation of NH_4^+ concentrations.

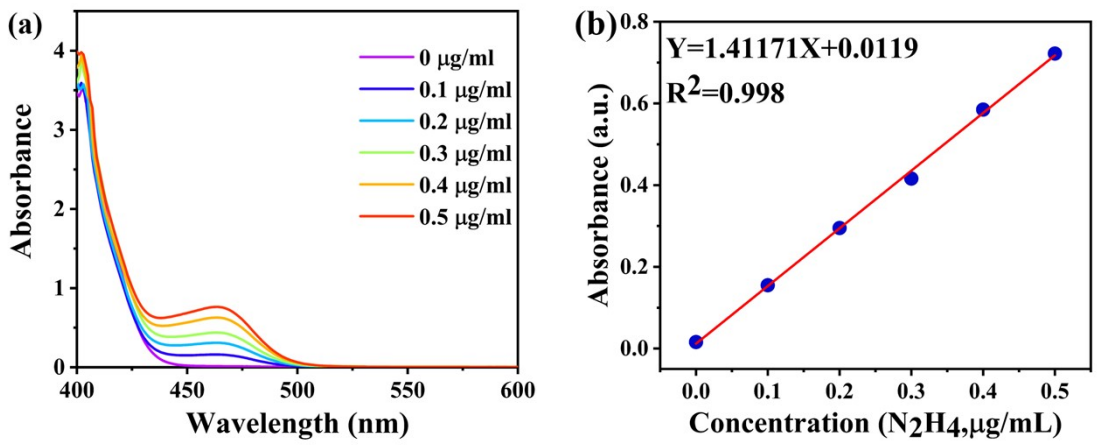

Figure S9 (a)UV-vis absorption spectrum of N_2H_4 quantitatively measured by Watt-chrisp method after incubated for 15 min at room temperature; (b) calibration curve of N_2H_4 measured by Watt-chrisp method.

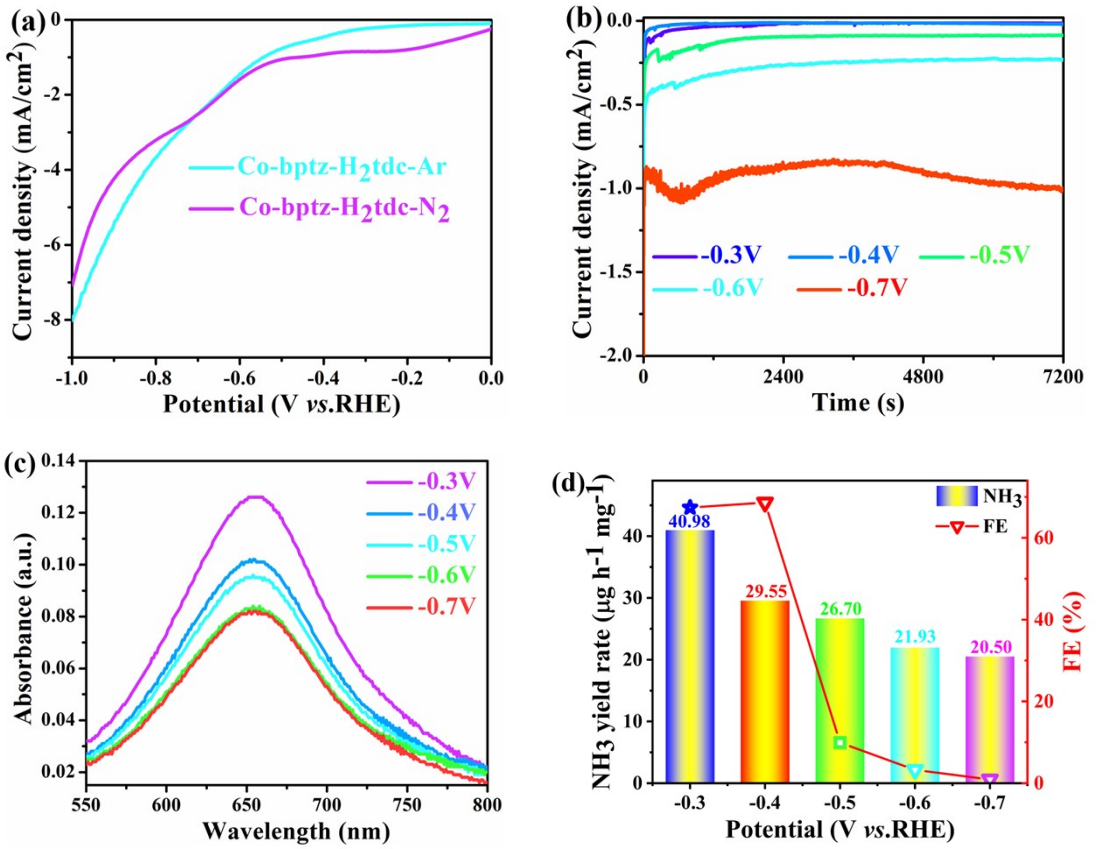

Figure S10 (a) Polarization curves of Co-bptz-H_2tdc in N_2 and Ar-saturated 0.1M Na_2SO_4 electrolyte; (b) Time-dependent current densities curves of Co-bptz-H_2tdc at

different potentials from -0.3 V to -0.7 V; (c) UV-vis spectra were estimated with the indophenol blue method at five given voltages for Co-bptz-H_2tdc; (d) NH_3 yield and FE of Co-bptz-H_2tdc at different potentials from -0.3V to -0.7V.

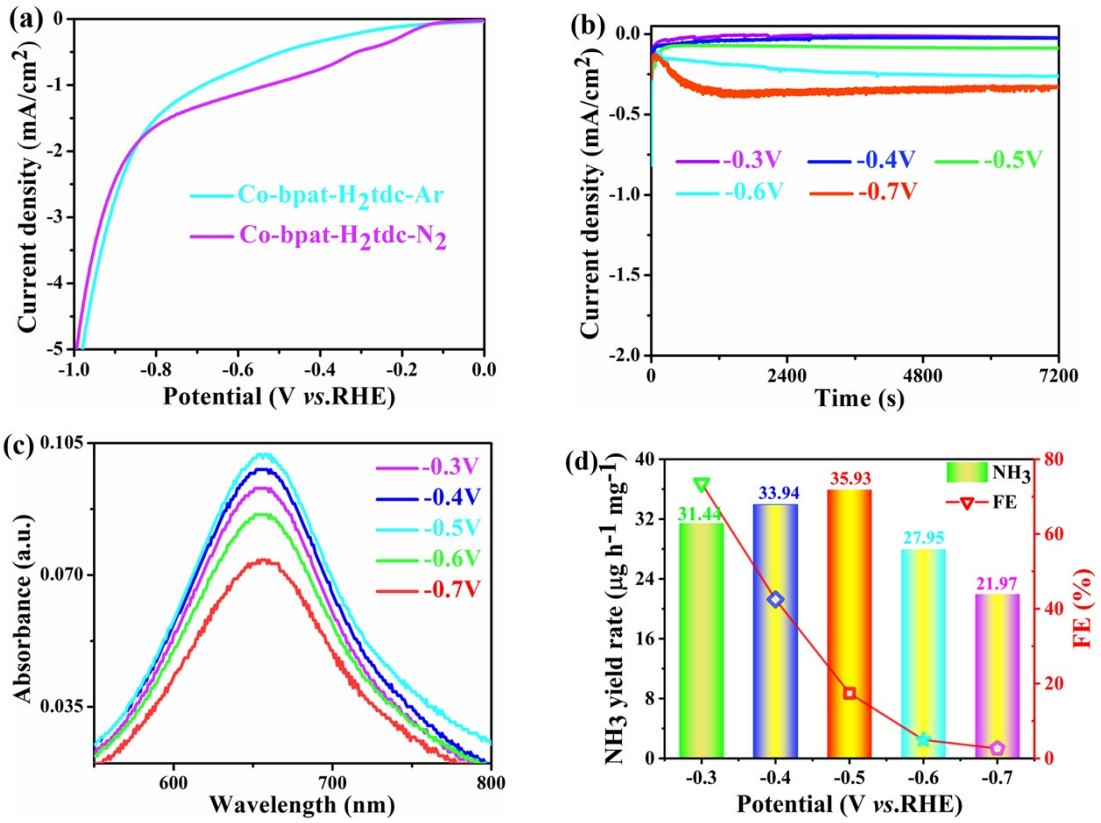

Figure S11 (a) Polarization curves of Co-bpat-H_2tdc in N_2 and Ar-saturated 0.1M Na_2SO_4 electrolyte; (b) Time-dependent current densities curves of Co-bpat-H_2tdc at different potentials from -0.3 V to -0.7 V; (c) UV-vis spectra were estimated with the indophenol blue method at five given voltages for Co-bpat-H_2tdc; (d) NH_3 yield and FE of Co-bpat-H_2tdc at different potentials from -0.3V to -0.7V.

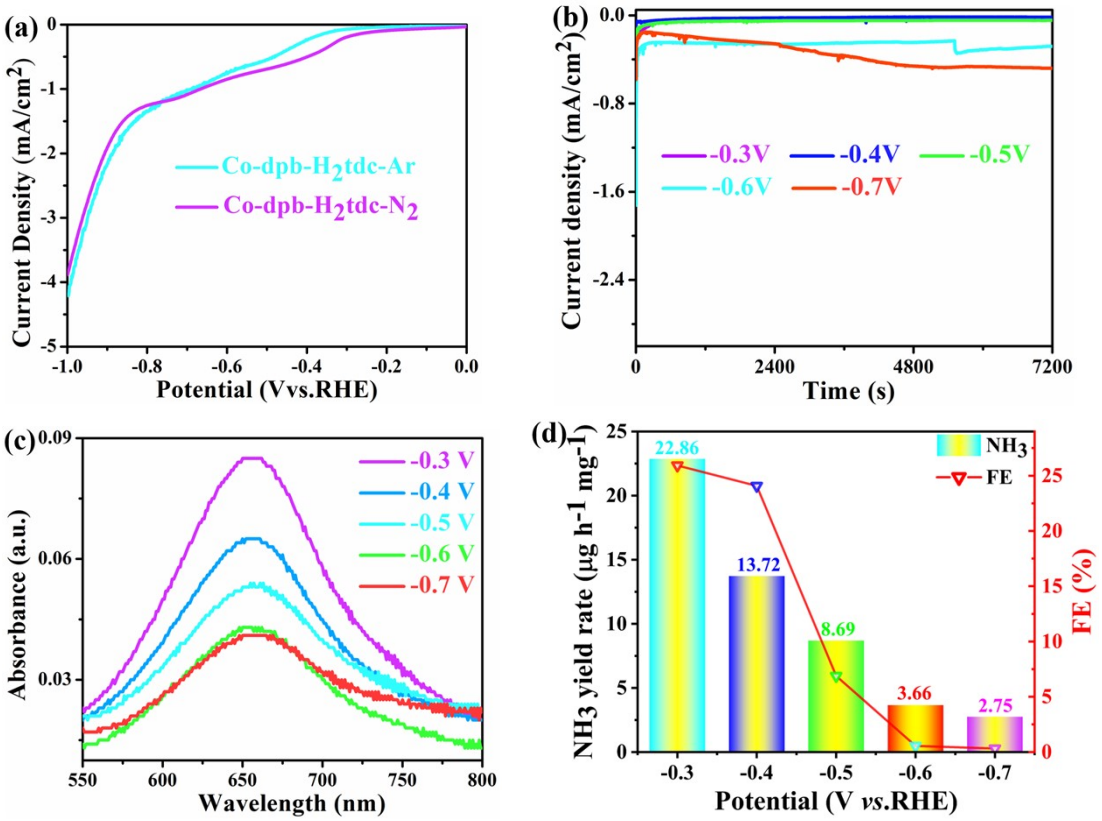

Figure S12 (a) Polarization curves of Co-dpb-H_2tdc in N_2 and Ar-saturated 0.1M Na_2SO_4 electrolyte; (b) Time-dependent current densities curves of Co-dpb-H_2tdc at different potentials from -0.3 V to -0.7 V; (c) UV-vis spectra were estimated with the indophenol blue method at five given voltages for Co-dpb-H_2tdc; (d) NH_3 yield and FE of Co-dpb-H_2tdc at different potentials from -0.3V to -0.7V.

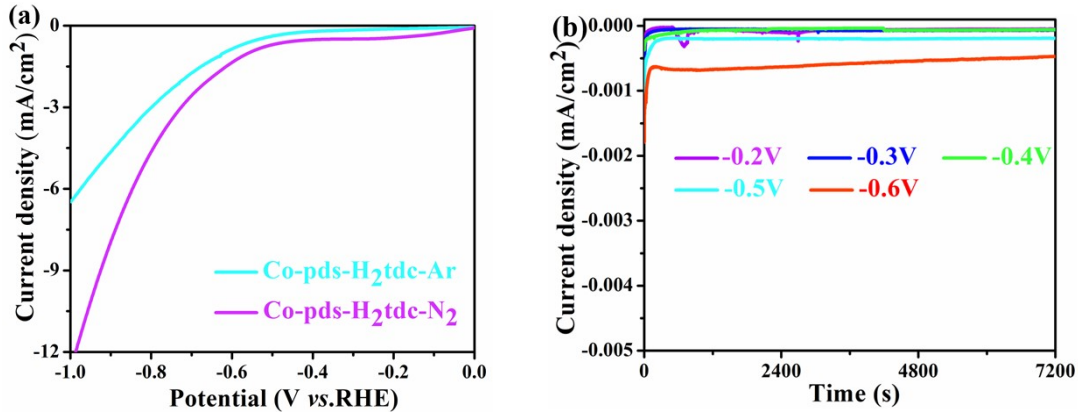

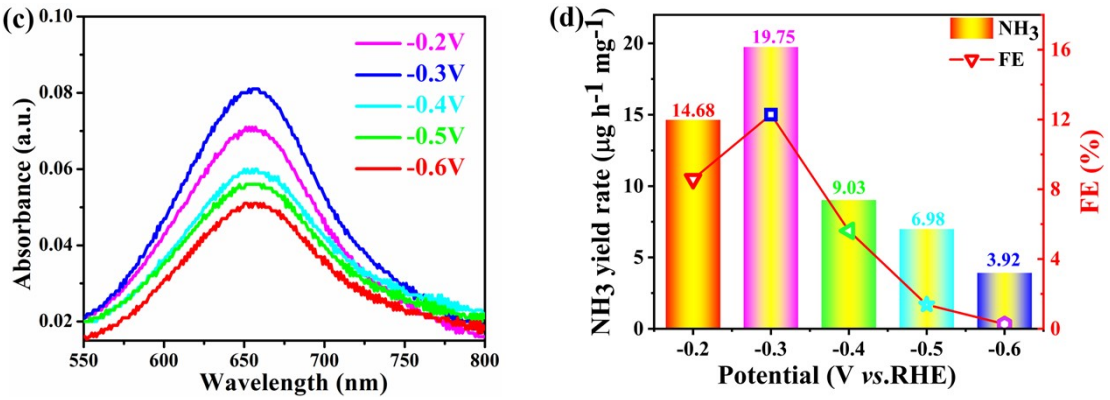

Figure S13 (a) Polarization curves of Co-pds-H_2tdc in N_2 and Ar-saturated 0.1M Na_2SO_4 electrolyte; (b) Time-dependent current densities curves of Co-pds-H_2tdc at different potentials from -0.2 V to -0.6 V; (c) UV-vis spectra were estimated with the indophenol blue method at five given voltages for Co-pds-H_2tdc; (d) NH_3 yield and FE of Co-pds-H_2tdc at different potentials from -0.2 V to -0.6 V.

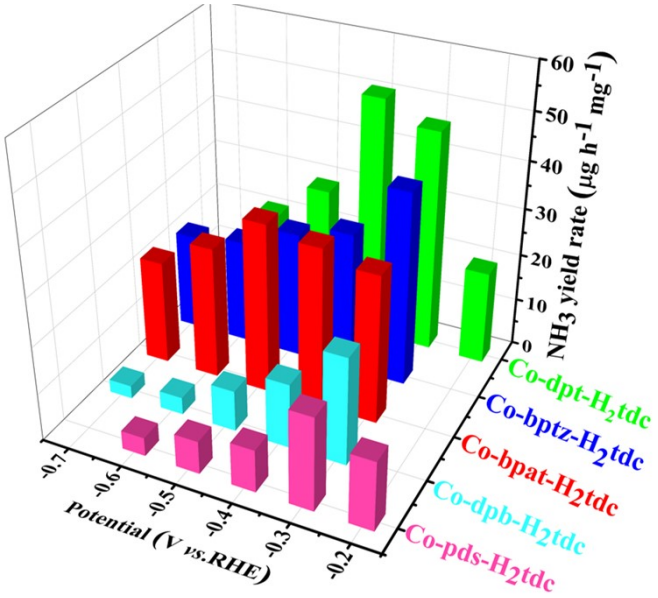

Figure S14 Comparison of NH_3 yield of Co-dpt-H_2tdc, Co-bptz-H_2tdc, Co-bpat-H_2tdc, Co-dpb-H_2tdc, Co-pds-H_2tdc.

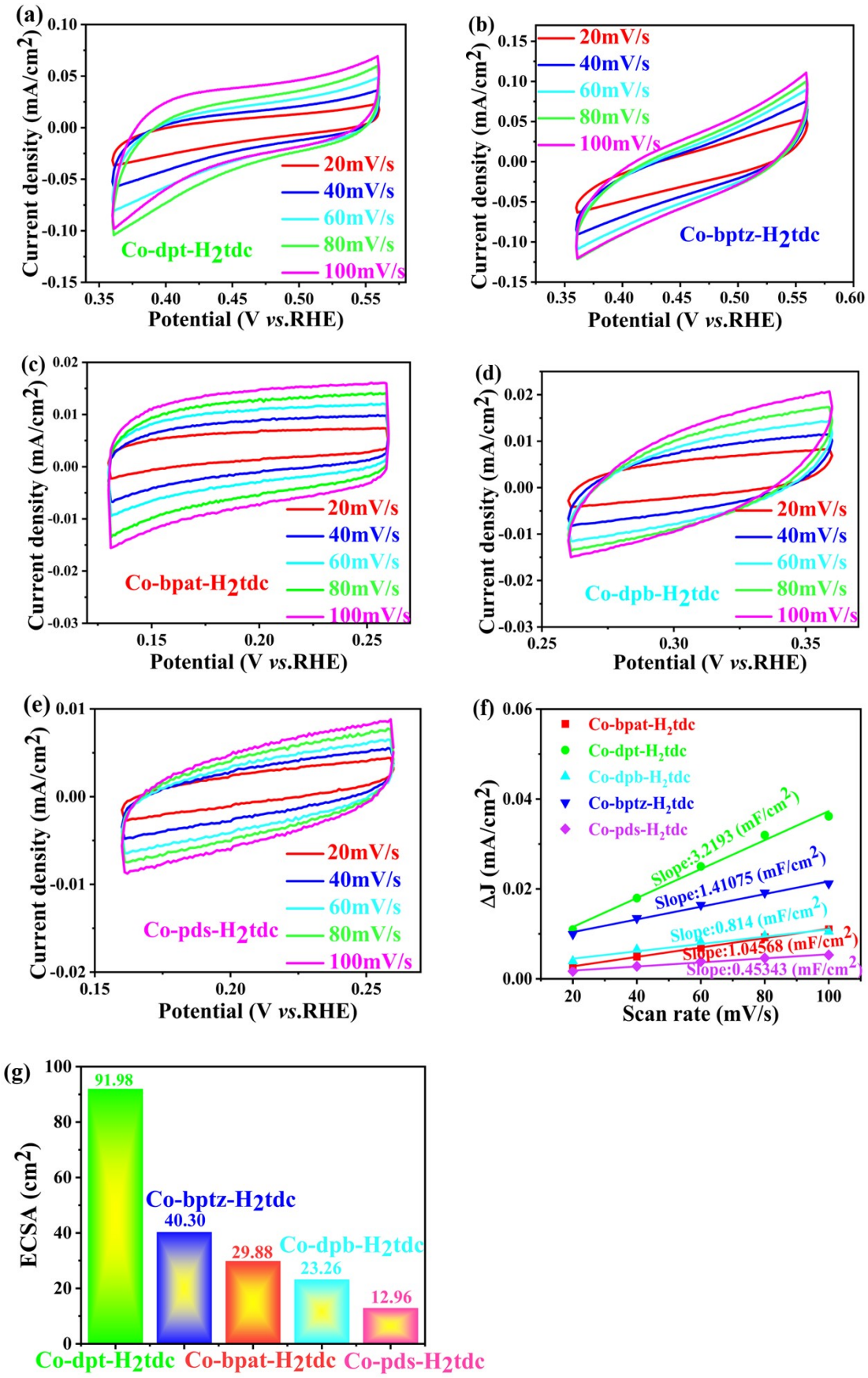

Figure S15 The CV of (a) Co-dpt-H_2tdc; (b) Co-bptz-H_2tdc; (c) Co-bpat-H_2tdc; (d) Co-

dpb-H_2tdc; (e) Co-pds-H_2tdc with different sweep speed; (f) C_{dl} corresponding to the five catalysts; (g) ECSA corresponding to the five catalysts.

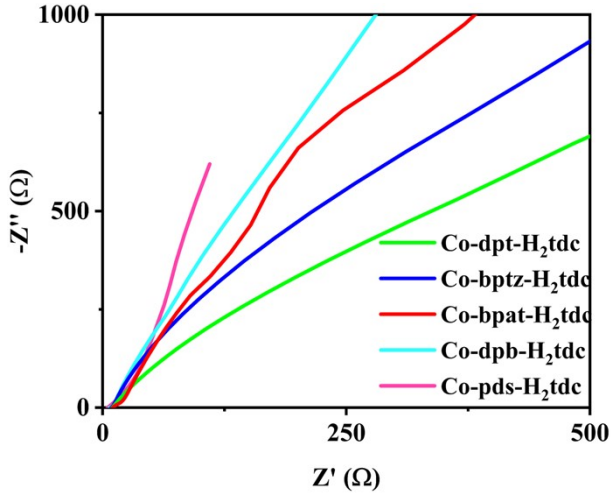

Figure S16 The EIS corresponding to the five catalysts.

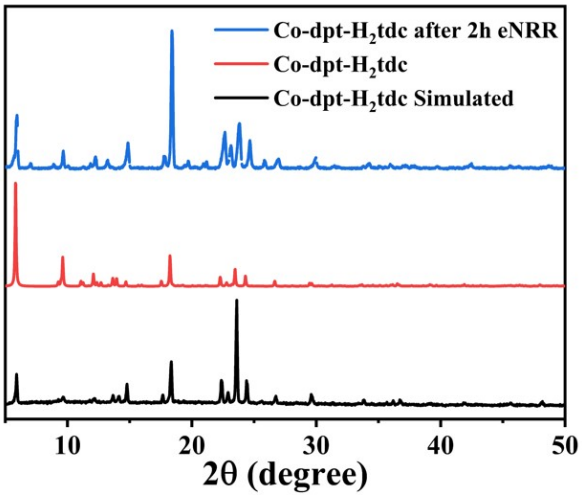

Figure S17 PXRD of Co-dpt-H_2tdc before and after eNRR electrocatalysis and standard spectra simulated.

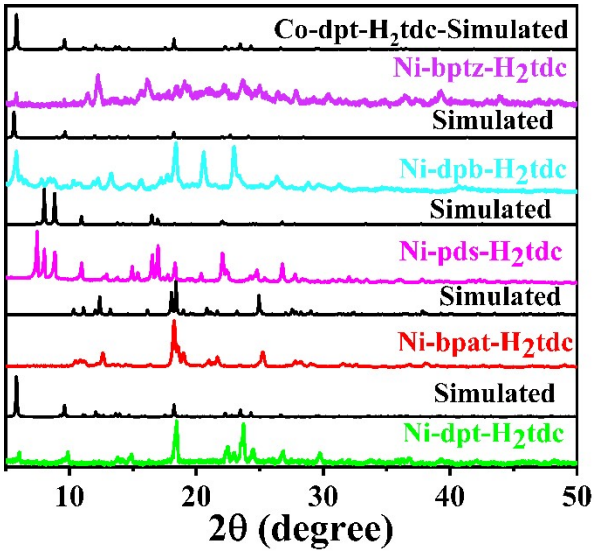

Figure S18 Comparison of standard spectra simulated by single-crystal diffraction data with PXRD of five Ni-MOFs.

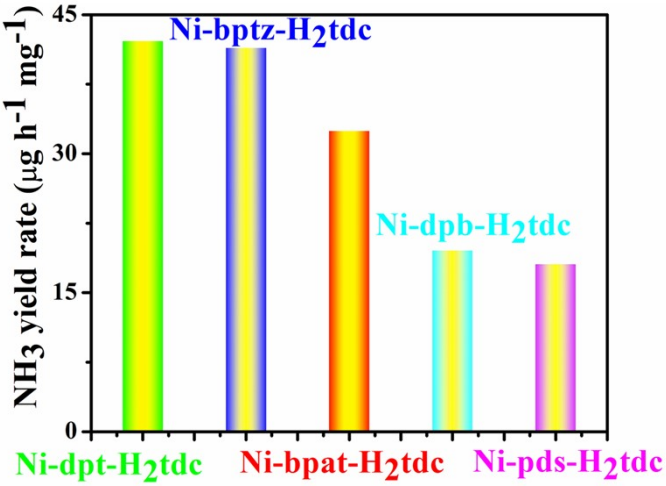

Figure S19 NH_3 yield rate at optimum voltage for five Ni-MOF catalysts.

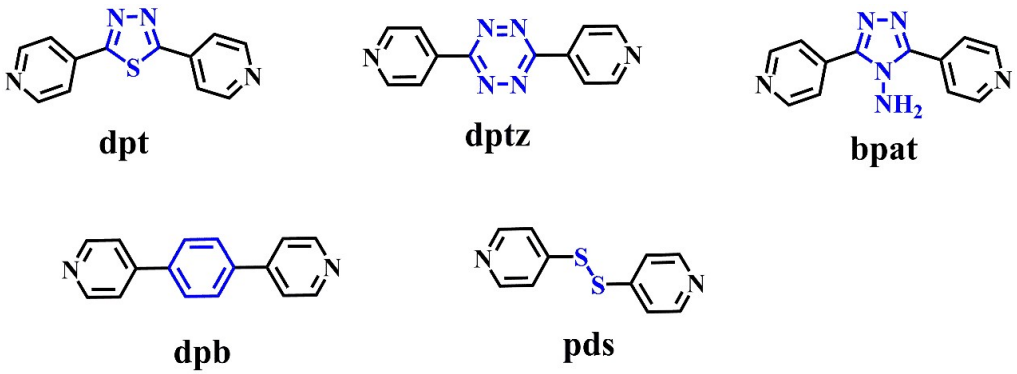

Figure S20 The structures of ligands.

Table S2 Crystallographic data and structure refinement details.

Crystal	Co-dpb-H_2tdc	Co-dpt-H_2tdc	Co-bpat-H_2tdc	Co-pds-H_2tdc
Formula	$C_{44}Co_2N_4O_8S_2$	$C_{36}H_{20}Co_2N_8O_8S_4$	$C_{22}H_{23}CoN_7O_6S$	$C_{32}H_{22}Co_2N_4O_9S_6$
Formula Weight	894.46	938.70	572.46	916.76
Crystal System	monoclinic	monoclinic	hexagonal	orthorhombic
Space group	$P2_1/c$	$P2_1/c$	$P6_1$	$C222_1$
a/Å	15.7170(17)	15.156(3)	9.8884(3)	16.8320(14)
b/Å	18.306(3)	18.378(2)	9.8884(3)	14.5894(16)
c/Å	16.1574(19)	15.9626(18)	42.8119(13)	23.725(3)
α/deg	90	90	90	90
β/deg	94.027(11)	91.834(12)	90	90
γ/deg	90	90	120	90
V/Å	4637.3(11)	4443.9(11)	3625.3(3)	5826.1(11)
Z	4	4	6	4
D(calc) [g/cm^3]	1.281	1.403	1.573	1.045
Mu (MoKa) [/mm]	0.856	0.989	0.851	0.821
F (000)	1768	1896	1770	1856
Temperature (K)	293	293	293	293
Theta Min-Max	2.1, 25.0	3.4, 25.0	2.4, 25.0	3.4, 25.0
Tot., Uniq. Data	20061, 8161	7788, 7788	16548, 4242	17266, 5117
R(int)	0.101	0.000	0.057	0.062
Observed Data	2195	4039	3900	4332
Nref, Npar	8161, 541	7788, 523	4242, 338	5117, 241
R	0.1733	0.1141	0.0504	0.0962
wR_2	0.4908	0.3041	0.0951	0.2921
S	1.06	1.02	1.10	1.13
Max. and Av. Shift/Error	0.28, 0.03	0.00, 0.00	0.00, 0.00	0.00, 0.00
Min. and Max. Resd. Dens. [e/Å^3]	-1.31, 3.59	-0.83, 3.10	-0.65, 0.56	-0.74, 1.60

Table S3 Selected bond lengths (Å) and angles (deg) for Co-MOFs

Co-dpb-H_2tdc			
Co1-O1	2.085(13)	O3-Co1-N1	89.1(5)
Co1-O3	2.011(10)	O3-Co1-N2a	88.1(5)
Co1-O5	2.051(11)	O5-Co1-N1	91.5(5)
Co1-N1	2.151(11)	O5-Co1-N2a	87.3(5)
Co1-N2a	2.125(14)	N1-Co1-N2a	176.1(5)
Co2-O4	2.038(13)	O4-Co2-O6	117.9(5)
Co2-O6	2.020(10)	O4-Co2-N3	89.8(5)
Co2-N3	2.182(11)	O4-Co2-N4a	90.5(5)
Co2-N4a	2.164(14)	O4-Co2-O7b	92.5(5)
Co2-O7b	2.096(13)	O4-Co2-O8b	150.5(4)
Co2-O8b	2.377(13)	O6-Co2-N3	86.2(5)
O1-Co1-O3	150.1(5)	O6-Co2-N4a	91.0(4)
O1-Co1-O5	92.6(4)	O6-Co2-O7b	149.5(5)
O7b-Co2-O8b	58.0(5)	O6-Co2-O8b	91.6(5)
O1-Co1-N1	93.6(5)	N3-Co2-N4a	177.0(5)
O1-Co1-N2a	90.2(5)	O7b-Co2-N3	90.9(5)
O3-Co1-O5	117.1(5)	O7b-Co2-N4a	92.1(5)
N3-Co2-O8b	89.9(5)	N4a-Co2-O8b	91.3(5)

Symmetry element: a = -1 + *x*, *y*, *z*; b = *x*, 3/2 - *y*, -1/2 + *z*.

Co-dpt-H_2tdc			
Co1-O1	2.032(6)	O5-Co1-N4b	90.9(2)
Co1-O5	2.094(6)	O5-Co1-O8c	149.3(2)
Co1-N1	2.104(8)	N1-Co1-N4b	175.9(3)
Co1-N4b	2.127(9)	N1-Co1-O6	90.2(3)
Co1-O8c	2.024(5)	N4b-Co1-O6	89.3(3)
Co1-O6	2.370(6)	O8c-Co1-N1	87.4(2)
Co2-O3d	2.402(6)	O8c-Co1-N4b	88.5(2)
Co2-O2	2.005(6)	O8c-Co1-O6	90.7(2)
Co2-N5	2.154(8)	O2-Co2-N5	85.9(3)
Co2-N8a	2.088(8)	O2-Co2-N8a	89.4(3)
Co2-O7c	2.015(6)	O2-Co2-O7c	117.2(2)
Co2-O4d	2.092(6)	O2-Co2-O4d	148.4(2)
O1-Co1-O5	93.6(2)	O7c-Co2-N5	90.9(3)
O1-Co1-N1	91.7(3)	O4d-Co2-N5	90.7(2)
O1-Co1-N4b	90.6(3)	O7c-Co2-N8a	92.4(3)
O1-Co1-O8c	117.1(2)	O4d-Co2-N8a	92.7(2)
O1-Co1-O6	152.1(2)	O2-Co2-O3d	90.2(2)

O5-Co1-O6	58.6(2)	N5-Co2-N8a	175.1(3)
O5-Co1-N1	92.3(2)	O4d-Co2-O7c	94.2(2)
O7c-Co2-O3d	152.5(2)	O4d-Co2-O3d	58.3(2)
N5-Co2-O3d	88.9(3)	N8-Co1-O3d	89.9(2)

Symmetry element: a = -1 + *x*, *y*, *z*; b = 1 + *x*, *y*, *z*; c = *x*, 1/2 - *y*, -1/2 + *z*; d = *x*, 3/2 -*y*, -1/2 + *z*.

Co-bpat-H_2tdc			
Co1-O1	2.217(4)	O1W-Co1-O2	151.80(16)
Co1-O1W	2.087(4)	O1W-Co1-N5	89.99(16)
Co1-O2	2.170(4)	O1W-Co1-N6	94.23(16)
Co1-N5	2.171(4)	O1W-Co1-O3a	98.10(15)
Co1-N6	2.152(4)	O2-Co1-N5	88.30(14)
Co1-O3a	2.023(4)	O2-Co1-N6	88.77(14)
O1-Co1-O1W	91.94(15)	O2-Co1-O3a	109.91(16)
O1-Co1-O2	60.16(16)	N5-Co1-N6	175.5(2)
O1-Co1-N5	94.43(18)	O3a-Co1-N5	86.85(17)
O1-Co1-N6	87.14(18)	O3a-Co1-N6	90.87(17)
O1-Co1-O3a	169.89(16)		

Symmetry element: a = *x*, -1 + *y*, *z*.

Co-pds-H_2tdc			
Co1-O1	2.084(6)	O5-Co1-N1	90.7(3)
Co1-O5	2.144(5)	O3c-Co1-O5	95.8(3)
Co1-N1	2.167(9)	O5-Co1-N2b	174.7(2)
Co1-O3a	2.059(7)	O4d-Co1-O5	87.8(2)
Co1-N2b	2.151(9)	O3c-Co1-N1	89.3(3)
Co1-O4c	2.086(7)	N1-Co1-N2b	94.0(3)
O1-Co1-O5	90.4(2)	O4d-Co1-N1	177.9(3)
O1-Co1-N1	90.1(3)	O3c-Co1-N2b	86.8(3)
O1-Co1-O3a	173.8(3)	O3c-Co1-O4c	92.3(3)
O1-Co1-N2b	87.1(3)	O4d-Co1-N2b	87.5(3)
O1-Co1-O4c	88.5(3)		

Symmetry element: a = -1/2 + *x*, 1/2 + *y*, *z*; b = 1/2 + *x*, 1/2 + *y*, *z*; c = 5/2 - *x*, 1/2 + *y*, 3/2 - *z*.

Table S4 Summary of the eNRR performances for reported electrocatalysts.

Catalysts	Electrolyte	NH_3 yield ($\mu g \cdot h^{-1} \cdot mg_{cat}^{-1}$)	FE (%)	Refs.
MoS_2@ZIF-71	0.1 M Na_2SO_4	56.69	30.91	28
βBi_2O_3-0.6	0.1 M Na_2SO_4	51.36	38.67	29
Co-dpt-H_2tdc	0.1 M Na_2SO_4	51.30	29.2	This work
HT Au@MOF	0.1 M Na_2SO_4	49.5	60.9	30
MoFe-PC	0.1M HCl	34.23	16.83	31
Co-TCPP	0.1 M HCl	28.3	11.58	32
PdCu@UiO-S@PDMS	0.1 M HCl	20.24	13.16	37